

# Interaction among different spatio-temporal scale fluctuations through zonal flows

Y. Kishimoto,<sup>1)</sup> J.Q. Li,<sup>1)2)</sup> Y. Idomura,<sup>1)</sup> and A. Smolyakov<sup>3)</sup>

<sup>1)</sup> Naka Fusion Research Establishment, JAERI, Naka, Ibaraki 311-0193, Japan

<sup>2)</sup> Southwestern Institute of Physics, Chengdu, People's Republic of China

<sup>3)</sup> University of Saskatchewan, Saskatoon, S7N 5E2 Canada

E-mail: kishimoy@fusion.naka.jaeri.go.jp

**Abstract.** Zonal flows generated by fluctuations on some scale are expected to affect fluctuations on other different spatial-temporal scales in addition to regulating their own fluctuation. As an example, here we discuss ITG turbulence embedded in a small scale ETG-driven zonal flow based on 3-dimensional gyro-fluid simulations. At first, we identified the ETG-driven zonal spectrum and found that the zonal flows are enhanced in higher pressure and lower magnetic shear plasma, leading to a self-organized high energy state. Further, we found a new suppression mechanism of the long wavelength ITG mode by the small-scale ETG-driven zonal flows, namely, the radially non-local mode coupling and the associated energy transfer. Besides the role of suppression in ITG turbulence, we have for the first time observed intermittent and/or bursting behavior in the ion heat transport originating from the complicated mutual interaction among ETG-driven zonal flows, ITG turbulence, and the associated ITG-driven zonal flows.

## 1 Introduction

It is widely recognized that various profile formation in tokamaks is tightly coupling with various radial electric fields and related flow generation[1]. Besides neoclassically driven equilibrium flows, turbulence self-generated  $\vec{E} \times \vec{B}$  zonal flows have been shown to play an efficient role in regulating the turbulence structure and suppressing the heat transport in magnetized plasmas[2-4]. In tokamaks, there exist many types of fluctuation with a spatial scale from micro-scale electron gyro-radius to macro-scale machine size. Since the zonal flows are generated through nonlinear interaction of the turbulence, different scale zonal flows may be simultaneously generated in the plasma. Since the zonal flows are characterized by large spatial structures in both the toroidal and poloidal directions and long auto-correlation times, it is expected that the zonal flows generated by fluctuations on some scale may affect fluctuations on other different scales in addition to regulating their own fluctuation level [5,6]. The interaction mechanism, nonlinear dynamics and/or turbulent transport affected by such small-scale flows are open issues. Note that a direct interaction has been considered based on the viscosity damping mechanism[7].

In this paper, we exploit a new role of zonal flows in regulating different spatio-temporal scale turbulence and the relevant transport, and further aim at studying the indirect interaction between the different scale turbulences through zonal flows. As an example, here we investigate the ion temperature gradient (ITG) turbulence embedded in the micro-scale zonal flows driven by electron temperature gradient (ETG) turbulences based on our theory and gyro-fluid simulations. This topic involves the interaction between small-scale sheared flows, for example, with a spatial scale on electron gyro-radius or the collisionless skin depth, and the large-scale turbulence. Such effects may sensitively depend on the zonal flow spectrum, which is typically characterized by the auto-correlation length (or

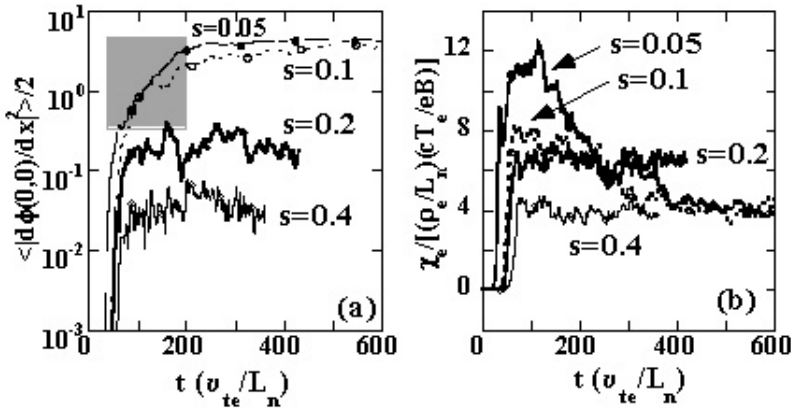


FIG. 1. Evolution of zonal flow energy (a) and electron heat diffusivity  $\chi_e$  (b) for different magnetic shears. Shadow corresponds to zonal flow instability region

typically the radial wavelength) and auto-correlation time. In order to identify the spectrum, at first we perform the gyro-fluid simulations of the ETG turbulence-zonal flows system. The ETG-driven zonal flows are believed to be generally very weak compared with the background turbulence and hardly work for suppressing the turbulent electron transport contrary to the ITG counterpart[8]. However, we found that weak magnetic shear induces the large amplitude zonal flows in steeper electron temperature gradient regime. As a result, the ETG turbulence-zonal flow system may be self-organized to a higher energy state with lower electron transport level. We have developed a theoretical model based on the modulational instability analysis and found that the weak shear is favorable to the zonal flow instability and higher saturation level.

Based on the knowledge of the ETG-driven zonal flows, we performed the ITG turbulence simulation including the effect from such micro-scale zonal flows. So far, discussions for flow shearing stabilization is focused on the sheared flows with  $k_x^{(z)} \leq k_x^{(turb)}$  ( $k_x^{(z)}$  and  $k_x^{(turb)}$  are typical radial value number of zonal flows and turbulence, respectively)[9]. We have found a new suppression mechanism of the long wavelength ITG mode by the small-scale flows through the radially nonlocal mode coupling[6]. Besides the role of suppression in ITG turbulence, we have for the first time observed intermittent and/or bursting behavior in the ion heat transport originating from the complicated mutual interaction among ETG-driven zonal flows, ITG turbulence, and the associated ITG-driven zonal flows.

## 2 Zonal flow control by magnetic shear and electron transport reduction

The generation of ETG-driven zonal flows has been found to be a slower process[8]. However, here we demonstrate that the zonal flows can be enhanced by controlling the magnetic shear and pressure gradient. Our simulations are based on a 3-dimensional gyro-fluid electrostatic slab model with the Landau damping and adiabatic ion response[8,10], considering that the electron transport is essentially electrostatic even though the electromagnetic effect seems an important component [11,12]. In order to understand the electron transport with electron ITB, the simulations are focused on the experimental observations, which are characterized by the steep electron temperature gradient,  $\eta_e = L_n/L_{Te}$ , and weak magnetic shear  $\hat{s} = L_n/L_s$  [13,14]. The typical parameters are  $\mu_\perp = \eta_\perp = \chi_\perp = 0.5$ ,  $L_x = 100\rho_e$ ,  $L_y = 10\pi\rho_e$ ,  $L_z = 2\pi L_n$ ,  $m_{Max} = 24$ , and a periodic (twisting) boundary condition is employed in the radial direction.

Figure 1 shows the results illustrating the time history of electron heat diffusivity  $\chi_e$  and corresponding zonal flow energy  $\langle |d\phi^{(z)}/dx|^2 \rangle$  for different magnetic shears in the case of  $\eta_e = 6$ . ETG fluctuations exponentially grow up and surely saturate at different levels with corresponding zonal flows as the magnetic shears decreasing. In the moderate

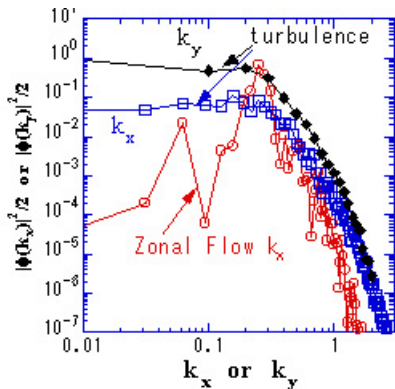


FIG. 2. Instantaneous spectra of both ETG turbulence and zonal flows at  $t = 600$  in the case of  $s = 0.1$  and  $\eta_e = 6$ .

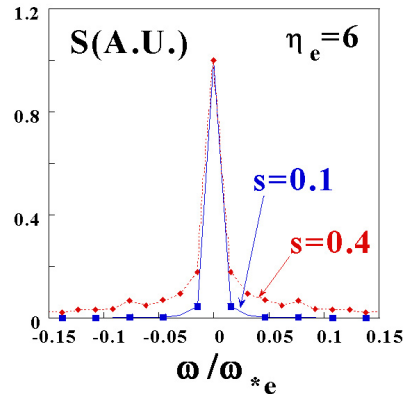


FIG. 3. Frequency power spectrum of zonal flows for different magnetic shears in the case of  $\eta_e = 6$ .

magnetic shear case, i.e.  $\hat{s} = 0.4$  and  $0.2$ , the zonal flows are weak compared with the dominant turbulent component and has no effect on the saturation and suppression of the ETG turbulence. When the magnetic shear is further weakened to  $\hat{s} = 0.1$ , the linear ETG-drive and then the saturation level of the fluctuations increase. However, after the saturation, the heat diffusivity is found to be gradually decreased, reaching to a lower quasi-steady state level. The tendency is more prominent in the case of  $\hat{s} = 0.05$ . Noticeably, the zonal flows undergo a growing phase (shadow part) in accordance with the decrease of the heat diffusivity, approximately exponential, after the saturation. This growing phase shows a zonal flow instability, namely, turbulent fluctuations could be converted to large amplitude zonal flows. The turbulence ( $k_x, k_y$ ) and zonal flow  $k_x^{(z)}$  spectra are shown in Fig.2. It is clearly seen that the zonal flow spectrum reveals a narrow peak around  $k_x^{(z)} = 0.2 - 0.3$  with high amplitudes, which are almost same level as that of background turbulences, implying that the turbulences are strongly self-regulated by the zonal flows. The frequency power spectra of the zonal flows are also shown in Fig.3 for moderate and weak shear cases, i.e.  $\hat{s} = 0.4$  and  $\hat{s} = 0.1$ . The power spectra show a strong peak at  $\omega = 0$  with the typical auto-correlation frequency  $\Delta\omega$  that is much lower than the electron diamagnetic frequency  $\omega_{*e}$ , typically  $\Delta\omega/\omega_{*e} \leq 0.01$ . It is also found that the auto-correlation time becomes longer for the weaker magnetic shear, suggesting that the coherence of the zonal flows is more pronounced at higher amplitude regime.

We now present a simple analysis based on Hasegawa-Mima (H-M) equation [15]

$$(1 - \nabla_{\perp}^2) \partial_t \phi = \partial_y \phi + [\phi, \nabla_{\perp}^2 \phi], \quad (1)$$

which can demonstrate that the weak shear is favorable to the zonal flow instability. Zonal flows can be generated in turbulence only through the nonlinear interaction [15-17]. Previous modulational analyses were mainly based on an universal treatment by assuming a monochromatic wave packet. Actually, the different turbulence is characterized by the specific eigen-mode structure and fluctuating property, which involve the essentially magnetic shear dependence. Hence, we should take the slab ETG eigen mode as a pump to drive zonal flows. In a general slab drift wave theory, the eigen structure of the lowest order radial mode in the fluid limit is described as  $\hat{\phi}(x) \sim \exp(-i\sigma x^2)$  (here  $\sigma = L_n |\hat{s}| / 2\Omega R q$ ) with the normalized (by  $\omega_{*e}$ ) complex eigen value  $\Omega \sim (-1, 1) \sqrt{\hat{s}}$  for given  $\eta_e$  and  $k_y$ .

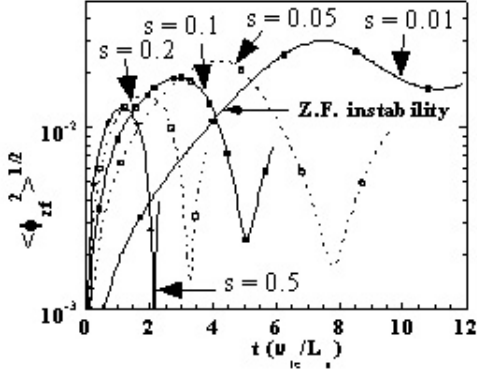


FIG. 4. Modulational zonal flow instability for the slab ETG eigenmode type pumping wave for  $k_y \rho_e = 1.0$  for different magnetic shears.

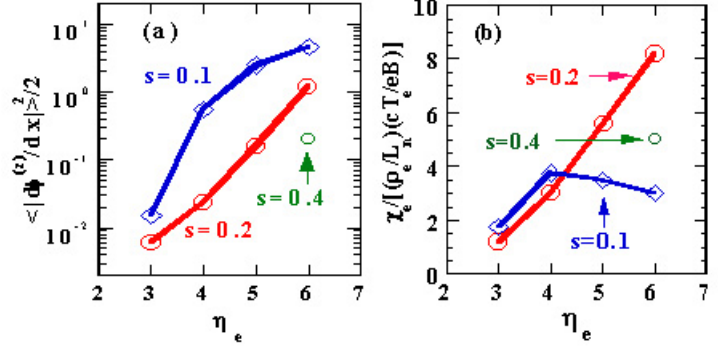


FIG. 5. Scan of zonal flow energy (a) and electron heat diffusivity  $\chi_e$  (b) for different  $\eta_e$  and  $\hat{s}$ .

This pumping wave is written as [8]

$$\phi_p(t, x, y) = \phi_0(t) \exp(-i\sigma x^2) \cos(k_y y). \quad (2)$$

It seems difficult to get an analytical dispersion relation and evolution equation of zonal flow instability similar to the previous derivations [8,16] due to the radial mode structure of pumping wave. Considering that the modulational processes are the same, we could use a summed dispersion relation for all  $k_x$  components and given zonal flow  $k_q$  [8]

$$\omega^2 = \sum_{k_x} \frac{k_y^2 k_q^4 (k_x^2 + k_y^2 - k_q^2) (3k_x^2 - k_q^2 - k_y^2) \phi_{k_x}^2}{4\Lambda_q [\Lambda_y + (k_x + k_q)^2] [\Lambda_y + (k_x - k_q)^2]}, \quad (3)$$

with  $\Lambda_{q,y} = 1 + k_{q,y}^2$  to approximately understand the shear dependence of zonal flow instability. The increase of the radial mode width as the shear decreasing corresponds to a shrinking structure in Fourier  $k_x$  space. Small  $k_x$  can contribute to  $\omega^2 < 0$ , namely, excite zonal flow instability. We have directly calculated the H-M equation (1) by employing the pumping wave, Eq.(2). The modulational analysis could be also applied to the saturation mechanism of zonal flows. In order to probably compare the saturation levels of zonal flows for different shears, we fix the same total energy  $\int dx dy [\phi^2 + (\nabla \phi)^2] / 2$  of pumping waves in the calculations. Fig.4 plots the initial evolution of zonal flows for different shears. A zonal flow instability can be excited as the shear decreases. This is in well agreement with the above simple analysis. Further, the zonal flows also saturate at higher level as the shear becomes weak.

Combined with the results shown in Fig.1, the parametric scan of the magnetic shear and  $\eta_e$  dependence of the zonal flows and electron heat conductivities are studied as plotted in Fig.5. As  $\eta_e$  increases at the moderate magnetic shear  $\hat{s} = 0.2$ , the heat diffusivity increases together with the zonal flows, implying that the zonal flows are insufficient to suppress the electron transport. On the other hand, in the weak shear case around  $\hat{s} \leq 0.1$ , the heat diffusivity reaches the top at around  $\eta_e = 4$  and then shows a flat or rather decreasing tendency as  $\eta_e$  increases, exhibiting some transition nature. Note that the total fluctuation energy, i.e. the sum of turbulence part and zonal flow part keeps roughly constant or rather increasing, but the rate between turbulence part and zonal flow part is reversed, so that the turbulent dominated plasma is self-organized to a lower transport state with a higher zonal flows level.

This picture may be helpful to understand the characters of electron ITB behaviour observed in tokamak discharges with pure electron heating [13,14], although there also exist other mechanisms like MHD stability and TEM for the electron ITB physics [18,19]. The steeper electron temperature gradient, which may be locally driven by ECRH or other electron heating methods, can excite stronger ETG fluctuation. When the central  $q$  profile is controlled to become flat or reversed, the large amplitude zonal flows can be generated by the ETG turbulence and reduce the turbulences and electron heat transport.

### 3 ITG turbulent dynamics embedded in ETG-driven zonal flows

*Interaction mechanism:* From the analysis in Sec.2, large zonal flow potentials such as Mach number being about 0.5% with long-lived coherent structure have been observed. Those zonal flows developed with small spatio-temporal scale may be regarded as quasi-steady sheared fluid flows for ITG fluctuations. They can interact with large-scale turbulence on a gyro-phase averaged and velocity space averaged level from the view of fluid. Ignoring the weak time dependence, the coherent structure of the small-scale zonal flows are typically modeled by a circular function (sine or cosine) as follow,

$$v_{\perp p}(x) \propto d\phi_{ex}(x)/dx = A(k_{ex}) \cos(k_{ex}x), \quad (4)$$

when they are externally embedded in ITG fluctuations. Here,  $k_{ex}$  is the wave-number of small-scale flows normalized by ion gyro-radius, which is usually larger than 1. It is assumed that the factor  $A(k_{ex})$  has included both gyro-phase and velocity space averaging for the convenience of fluid treatment, in which  $k_{ex}$  dependence should be involved in Bessel functions. A rigorous gyro-kinetic integral calculation was done in Ref.[5].

Analyses and simulations are based on a gyro-fluid model of electrostatic slab ITG turbulence [6,8], which includes the small-scale flows as an external source by adding  $\partial_x \phi_{ex} \partial_y \tilde{f}$  term to the corresponding moment equations. For usual ITG-driven zonal flows with  $k_x^{(z)} \leq k_x^{(ITG)}$ , the Doppler shift dominantly leads to local shearing of fluctuating potential structures. However, a different interaction mechanism for small-scale zonal flows can be advisably revealed by a perturbation analysis. Keeping the lowest order effects of a small amplitude flow and Fourier transforming the perturbed eigen-mode equation from real space to wave-number  $k$  space, i.e.,  $\phi(x) = \sum_k \phi_k \exp(-ikx)$ , it can formally yield

$$(\mathcal{L} + U_k)\phi_k = A\vartheta(\Lambda - \mathcal{L})(\phi_{k+k_{ex}} + \phi_{k-k_{ex}}). \quad (5)$$

Here,  $\mathcal{L} \equiv d^2/dk^2$ ,  $U_k = (L_s\Omega/L_n)^2 [k_y^2 - (1-\Omega)/(\Omega+K) + k^2]$ ,  $\Lambda = L_s^2\Omega^3(1+K)/2L_n^2(\Omega+K)^2$ ,  $\vartheta = L_n/\Omega$  with  $\Omega = \omega/\omega_{*e}$  and  $K = 1 + \eta_i$ . This is a coupling equation system of different radial components  $k$ ,  $k + k_{ex}$ , and  $k - k_{ex}$ . It shows that small-scale sheared flows can produce radial mode coupling of different harmonics, which is formally similar to the well-known poloidal coupling of drift wave in a toroidal configuration. However, the new feature of this model is that the coupling is non-local in the radial spectral space due to  $k_{ex} > 1$ , generally. It may directly transfer the fluctuating free energy from the unstable longer wavelength region, to stable or damped components at shorter wavelengths. Then, the ITG mode is expected to be stabilized. This non-local coupling sensitively depends on two factors: ① the intensity of small-scale flows including gyro-phase averaged effects, which may strongly reduce the coupling intensity due to in the Bessel function dependence of  $k_{ex}$ , i.e.,  $A(k_{ex}) \sim A_0\Gamma_0^{1/2}$ ,  $\Gamma_0 = I_0(k_{ex}^2) \exp(-k_{ex}^2)$  [20], and ② the spectral structure of ITG fluctuations between different radial modes  $k$ ,  $k + k_{ex}$ , and  $k - k_{ex}$ . The latter means that the smaller the decay rate of ITG turbulence spectrum is in the inertial range, the

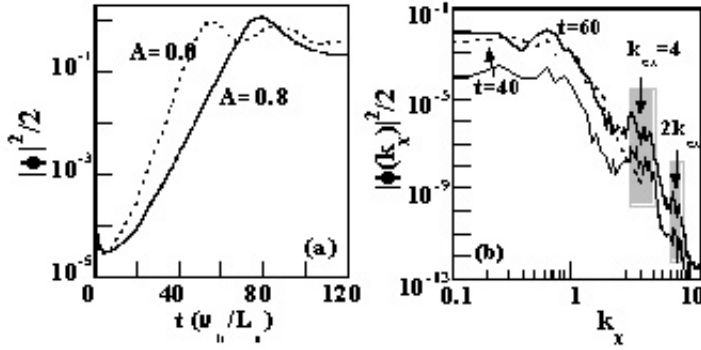


FIG. 6. The time history of fluctuation energy (a) and instantaneous radial spectra (b) without (dashed) and with (solid) small-scale flows.

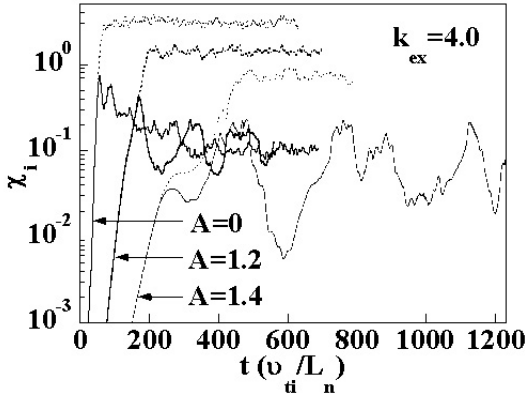


FIG. 7. The time history of  $\chi_e$  for different small-scale flows. Dashed curves correspond to their counterparts artificially excluding ITG-generated zonal flows.

stronger the coupling is for a given  $k_{ex}$ . It can be expected that the zonal flows generated by the mesoscale turbulence on the collisionless skin depth size may more effectively interact with ITG turbulence.

Nonlinear simulations have been performed by initially including small-scale flows for different flow intensities or wave-numbers  $k_{ex}$  [6]. The typical parameters are  $\eta_i = 2.5$ ,  $\hat{s} = L_n/L_s = 0.2$ ,  $\mu_\perp = \eta_\perp = \chi_\perp = 0.5$ ,  $L_x = 50\rho_i$ ,  $L_y = 10\pi\rho_i$ ,  $L_z = 2\pi L_n$ ,  $m \leq 15$ . Figure 6(a) shows the time evolution of the space averaged energy-like quantity  $\langle \phi^2 \rangle / 2$  in the earlier linear phase and the corresponding instantaneous radial spectra without and with small-scale zonal flows. An initial slowdown of the time evolution of the potential fluctuations is observed because of the stabilization role of small-scale flows. Most importantly, a spectral prominence with width  $\Delta k_x \sim 2$  clearly appears near  $k_x = k_{ex}$  as well as another one near  $k_x = 2k_{ex}$ , as shown in Fig.6(b). The monotonic decay spectrum is broken down at shorter wavelengths due to the radially non-local mode coupling. The width of the spectral prominence mirrors the fact that the unstable ITG mode stands in the range  $k_x \leq 1$ . Therefore, we conclude that small-scale zonal flows interact with large-scale ITG modes dominantly through the radially non-local mode coupling rather than the usual shearing decorrelation.

*Ion transport intermittency:* Our nonlinear simulations are designed to explore the role of small scale flows in ion heat transport. For a strong ITG turbulence drive, for example,  $\eta_i \geq 4$ , simulations show that even for the strongest small-scale flows, the small-scale zonal flows add less effects to the saturation level and the nonlinear evolution of ITG turbulence. As the turbulence drive is reduced, such as to  $\eta_i \leq 2.5$ , the corresponding levels of ITG fluctuations and self-generated zonal flows decrease much, as shown in Fig.7. Meanwhile, a remarkable intermittent or bursting behavior of ion heat transport appears, accompanied by the intermittent ITG-generated zonal flows with a time lag. It is also observed that the turbulence intensity  $\langle \phi^2 \rangle / 2$  and ion heat conductivity  $\chi_i$  are in phase during bursts [21]. The bursting period becomes longer, even infinite (it means no linearly unstable ITG modes) as the ETG-driven flows increase, as shown by solid curves

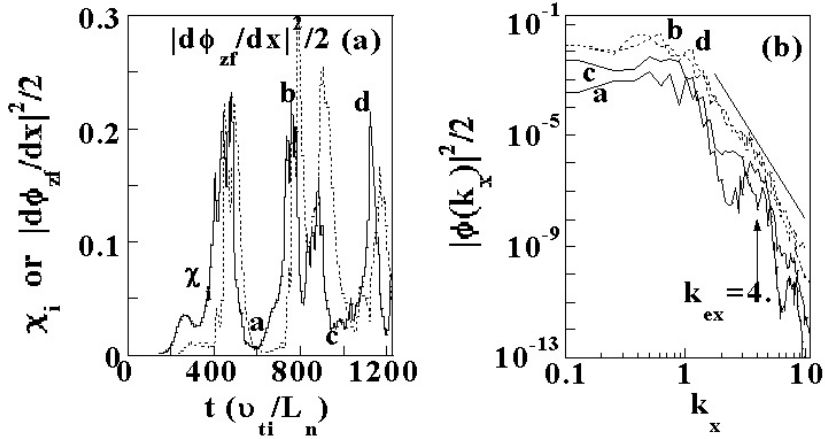


FIG. 8. The causal relation between transport and ITG-generated zonal flows(a) and the radial spectra at peaks and valleys of bursts(b).

in Fig.7. The time-averaged transport becomes decreasing for stronger flows. We next performed simulations by artificially excluding ITG-driven zonal flow components in order to find the related factors for the intermittency occurrence. The transport levels become about one order higher than their counterparts above and no any bursts are observed, as shown by the dashed curves in Fig.7. It is clear that the ITG-driven zonal flow dynamics still dominates the ITG turbulent transport in the relatively weak turbulence, but the turbulence can be remarkably modulated by small-scale flows. The emergence of ion transport intermittency requires the simultaneous presence of both small-scale flows and ITG-driven zonal flows.

The causal relation between the turbulent transport and ITG-generated zonal flows during bursts is plotted in Fig.8(a) for the case with  $A(k_{ex}) = 1.4$  in Fig.7. The bursting process can practically last long time (we have calculated to  $t = 3000$ ). How these small-scale zonal flows lead to an intermittent behavior in ITG turbulence is a key question. Note that the turbulent fluctuations seem to roughly exponentially go up and down during bursts, as shown in Fig.7. Performing spectral analyses for ITG turbulence, we found that at bursting peaks,  $k_x$  spectra are characterized by a monotonic decay structure with an approximate power law, which is a typical nonlinear Kolmogorov-type scaling. However, the spectral structures near  $k_x = k_{ex}$  and  $k_x = 2k_{ex}$  are gradually deformed after the bursts, actually degenerated to the linear spectral shape at valleys, as shown in Fig. 8(b), which is dominated by the linear nonlocal mode coupling. The bursts emerge in the recovery phases of nonlinear saturation spectra.

The physical mechanism of the intermittency may be understood as follows. At first, the exponentially growing ITG fluctuation is initially slowed down by small scale flows through nonlocal mode coupling, and saturated by self-generated zonal flows as well as the convective nonlinear coupling. Afterward, ITG fluctuation decreases due to the stabilization role of the micro-scale zonal flows, as a result of competition between nonlocal mode coupling and nonlinear inverse cascading. ITG-driven zonal flows follow the turbulent decreasing with a time log behind due to nonlinear drive decreasing. During this phase, the nonlinear turbulence spectrum is alternated to a linear deformed structure. When the effective shearing rate of ITG-generated zonal flows becomes lower than the turbulence decorrelation rate, the ITG fluctuations linearly grow up again and then lead to a burst.

## 4 Conclusion

In conclusion, our numerical experiments and analyses have shown that a large amplitude zonal flow can be sustained in strong electron pressure gradient with weak magnetic shears. The turbulent plasma can be self-organized to a higher confinement state with reduced heat transport. It suggests a probably controllable method of zonal flows in tokamak discharges by adjusting  $q$  profile. Note here that the Kelvin-Helmholtz instability excited in small  $k_y$  region is one of the candidate to suppress the strong zonal flows in addition to the modulational spectrum change, and further investigation is necessary[5]. Based on the knowledge of the ETG-driven micro-scale zonal flows, we have established a theoretic model on the interaction between different spatio-temporal scale fluctuations through zonal flows. A key physical mechanism of the interaction is found to be a radially non-local mode coupling between unstable and stable or damped components. It can deform the nonlinear monotonic decay spectrum of large-scale ITG turbulence in the inertial range and lead to an intermittent or bursting behavior of turbulent ion transport. These results open up a new paradigm where mutual interactions in the broad dynamic range of fluctuation spectrum including zonal components may provide crucial roles.

The authors thank to Dr. M.Azumi, Profs. M.Yagi, K.Itoh and J.Q.Dong for their fruitful comments and discussions. This work was supported by JAERI *NEXT Project*.

## References

- [1] ITOH, K. and ITOH, S-I., Plasma Phys. Cont. Fusion **38**, 1-49 (1996)
- [2] TERRY, P.W., Rev. Mod. Phys. **72**, 109(2000) and the references therein
- [3] DIAMOND, P.H., *et al.*, Nucl. Fusion **41**, 1047(2001)
- [4] LIN, Z., *et al.*, Science **281**, 1835(1998),
- [5] IDOMURA, Y., *et al.*, Nucl. Fusion **41**, 437(2000)
- [6] LI, J.Q. and KISHIMOTO, Y., Phys. Rev. Letts. **89**, 115002(2002)
- [7] ITOH, S-I. and ITOH, K., Plasma Phys. Cont. Fusion **43**, 1055(2001)
- [8] LI, J.Q. and KISHIMOTO, Y., Phys. Plasmas **9**, 1241(2001)
- [9] HAHM, T.S. and BURRELL, K.H., Phys. Plasmas **2**, 1648(1995)
- [10] HORTON, W., *et al.*, Phys. Fluids **31**, 2970(1988); Plasma Phys. Control. Fusion **13**, 207(1990)
- [11] DORLAND, W., *et al.*, Phys. Rev. Letts. **85**, 5579(2000)
- [12] JENKO, F., *et al.*, Phys. Plasmas **7**, 1904(2000)
- [13] BARBATO, E., Plasmas Phys. Control. Fusion **43**, A287(2001)
- [14] IDE, S., *et al.*, Plasmas Phys. Control. Fusion **44**, A137(2002)
- [15] HASEGAWA, A. and MIMA, K., Phys. Rev. Letts. **39**, 205(1977)
- [16] CHEN, L., *et al.*, Phys. Plasmas **7**, 3129(2000)
- [17] SMOLYAKOV, A.I., *et al.*, Phys. Rev. Letts. **84**, 491(2000)
- [18] GOHIL, P., Plasmas Phys. Control. Fusion **44**, A37(2002), also PARAIL, V.V., *ibid.*, A63
- [19] RAZUMOVA, K.A., *et al.*, Plasma Phys. Rep. **27**, 273(2001)
- [20] DORLAND, W., Ph.D thesis, Princeton University, 1993.
- [21] LIN, Z., *et al.*, Phys. Rev. Lett. **83**, 3645(1999)